Clin. Lab. 2025;71:XXX-XXX


## ORIGINAL ARTICLE

# Identifying *TP53* Copy Number Variations in Hematologic Malignancies with a Digital PCR Method

Wei Zhao [1, 3, 4], Dongming Yao [2, 3, 4], Qian Yuan [2, 3, 4], Jiang Lin [2, 3, 4], Di Yu [1, 3, 4], Jun Qian [1, 3, 4]

[1] *Department of Hematology, The Affiliated People's Hospital of Jiangsu University, Zhenjiang City, Jiangsu Province, P. R. China*
[2] *Laboratory Center, The Affiliated People's Hospital of Jiangsu University, Zhenjiang City, Jiangsu Province, P. R. China*
[3] *Zhenjiang Clinical Research Center of Hematology, Zhenjiang City, Jiangsu Province, P. R. China*
[4] *Institute of Hematology, Jiangsu University, Zhenjiang City, Jiangsu Province, P. R. China*

**SUMMARY**

***Background:*** ***Tumor protein p53*** **(*TP53*) is a well-known tumor suppressor gene, of which allelic status has widely been raising concern in recent years. Copy number (CN) loss in this gene results in either haploinsufficiency or loss of function. Though detection methods like next generation sequencing (NGS) or array-based comparative genomic hybridization (aCGH) can be applied, the accurate and cost-effective identification of copy number variation (CNV) remains a challenge for in-hospital laboratories.**

***Methods:*** **In this study, we developed a digital PCR method to quantify the *TP53* copy number in hematologic malignancies. Two Taqman probes were designed to be placed at the 5th and 7th exons of *TP53* gene, while another one was placed at the *RPP30* gene. By performing the experiments with the DNA of 102 healthy checkup individuals and two leukemia cell lines, we established the characteristics of the assay performance, including the limits of blank (LOB), the limits of detection (LOD), the linearities, and the coefficients of variation at the LOD levels. Forty-two samples from patients newly diagnosed with leukemia, lymphoma, myeloma, or myelodysplastic syndrome were further tested for validation. The results were then compared with other reports related to their allelic statuses of *TP53*.**

***Results:*** **The lower LOB of the exon 5 and exon 7 were revealed to be 1.756 and 1.836 copies per genome, respectively, while the upper limits were 2.008 and 2.041. The LOD for CN loss of two exons were 1.692 and 1.777 copies per genome, respectively. Taking NGS results as reference, 1.716 and 1.786 copies per genome for exon 5 and exon 7, respectively, were decided as the cutoff values for CN loss using the receiver operator curve (ROC) method. The areas under curve (AUC) for both exons reached 1.**

***Conclusions:*** **All in all, we consider dPCR an excellent tool for identifying *TP53* CNV status in hematologic malignancies.**

**(Clin. Lab. 2025;71:xx-xx. DOI: 10.7754/Clin.Lab.2024.241051)**

**Correspondence:**
Jun Qian
Department of Hematology
The Affiliated People's Hospital of Jiangsu University
8 Dianli Rd
Zhenjiang City
Jiangsu Province
P. R. China
Phone: + 86 51188915303
Email: qianjun0007@hotmail.com

Di Yu
Department of Hematology
The Affiliated People's Hospital of Jiangsu University
8 Dianli Rd
Zhenjiang City
Jiangsu Province
P. R. China
Phone: + 86 51188915301
Email: yudi0912@qq.com

Manuscript accepted November 6, 2024

**KEYWORDS**

digital PCR, TP53, copy number variation, hematologic malignancy

## INTRODUCTION

Copy number variation (CNV), as a subtype of structural variation, is commonly defined as the existence of an alteration in the copy number of a DNA segment that covers at least 1 kilobase when compared to the reference genome [1,2]. Such alterations contribute greatly to the functional abnormalities of the related genes in the cancer-associated scenarios. One typical example is the well-studied tumor suppressor gene *TP53*, which locates on the chromosome 17p13.1 and whose loss of function is considered most frequent in the events relating to human cancer, and a substantial part of this is driven by the mutation pattern that involves one missense mutation and one structure deletion on the other allele [3]. In the group of acute myeloid leukemia (AML) patients with *TP53* mutations, the incidence of harboring concurrent *TP53* copy number loss was reported to reach 70.2% [4]. For non-Hodgkin lymphoma patients, the reported frequency of chromosome 17p deletion was as high as 56% [3]. Given the impact that *TP53* copy number loss has on the prognosis and treatment choice of hematologic malignancies, multiple guidelines emphasize the detection and reporting of this genetic finding. For example, the 2019 recommendation from the American College of Medical Genetics and Genomics (ACMG) and the Cancer Genomics Consortium (CGC) has listed chromosome 17p or *TP53* deletion as Tier 1A genomic variants which encompasses those variants with the highest clinical significance [5]. Both the 5th edition of the World Health Organization (WHO) Classification of Hematolymphoid Tumors and the 2022 International Consensus Classification (ICC) of Myeloid Neoplasms and Acute Leukemias list MDS with biallelic inactivation/multi-hit mutations of *TP53* as a novel isolate diagnostic item. And the newly established molecular International Prognostic Scoring System for Myelodysplastic Syndromes (IPSS-M) also declared multi-hit *TP53* aberrations as top genetic predictor of adverse outcomes. The detection of *TP53* CNV will help in avoiding biallelic changes when only one mutation loci is found with a variant allele frequency (VAF) less than 50% [6-8]. Therefore, identifying whether *TP53* CNV exists has become an urgent need for clinical physicians.

Several methods have already been applied to assess the CNV statuses. Techniques like chromosome microarray analysis and next generation sequencing (NGS) are able to perform genome-wide assessment. But these techniques are expensive and platform dependent. Their sensitivities vary according to different platforms, algorithms, and loci that have been tested [9]. Fluorescence in situ hybridization (FISH) is a typical target-oriented CNV assessment, but the complexity of this method calls for well-trained technicians and the interobserver bias may not be ignored in the visual inspection steps. Apart from FISH, polymerase chain reaction (PCR) is another target-oriented method. Years ago, people made endeavors to use real-time quantitative PCR to detect CNVs, but soon found this approach to be inappropriate for handling the mosaicism of copy number state due to its large random errors within measurements [10]. Digital PCR (dPCR), however, is Poisson distribution based in nature. A single dPCR test nowadays involves at least tens of thousands of replicates isolated by small oil drops or chambers, providing an integrated digital output which largely eliminates the random errors within each replicate, and this digital output makes it possible to precisely determine the copies of targeted genes on an absolute scale [11].

In this study, we aimed to establish a dPCR approach to probe the copy number variations of *TP53* in hematologic malignancies. The performance characteristics of this approach have been assessed, verified, and compared with some existing CNV measurements.

## MATERIALS AND METHODS

### Study design

The aim of this study was to establish a solid, yet sensitive detection method for the screening of *TP53* CNV in hematologic malignancy samples. In pursuit of this aim, we started by designing the primers and probes of the target areas. The detection assay was optimized following the recommendations given in the digital MIQE guidelines [12]. Various primer and probe combinations, concentrations, and annealing temperatures were tested and compared. After determining the final assay, we verified the performance characteristics of the method following the guidance of the American National Committee for Clinical Laboratory's (NCCLS) protocol (EP17-A) [13]. Two critical values, limit of blank (LOB) and limit of detection (LOD), were determined and validated. Linearity properties of this method have also been tested. And finally, we verified the method's sensitivity and specificity by testing the samples from newly diagnosed patients with hematologic malignancies and comparing the test results with those from NGS tests or karyotyping. Two cutoff values were established as an alternative choice for the determination of copy number (CN) loss.

### Sample preparation

All the patients' samples involved were collected from April 2021 through June 2024 at the Affiliated People's Hospital of Jiangsu University. The 102 samples from healthy checkup individuals' peripheral blood all met the following conditions: 1) ≤ 70 years old; 2) no tumor-associated medical history; and 3) no abnormal blood routine test. Mononuclear cells were isolated from these samples by centrifugation and by applying

red cell lysis solution. DNA of these samples were extracted using the Puregene® Kits from QIAGEN company. Cryopreserved genome DNA samples isolated from blood or bone marrow from the patients with newly diagnosed hematologic malignancies were used. Two leukemia cell lines, SKM-1 and HL-60, were both NGS test verified to bear *TP53* deletions. The study was conducted in accordance with the Declaration of Helsinki and approved by the Ethics Committee and Institutional Review Committee of Jiangsu University Affiliated People's Hospital (ethical approval code: K-20240128-W; date of approval: 08-30-2024).

**Primers and probes**

Primers and probes were designed with the Oligo® primer analysis software v7. Two Taqman probes were placed over the DNA binding domain of *TP53* where splice mutations frequently happened [14], one at exon 5 and the other at exon 7. One probe was placed at the exon 7 of Ribonuclease P protein subunit p30 gene (*RPP30*), a housekeeping gene which is believed to be highly conserved and recommended by many to be used as a reference gene in PCR experiments [15]. All sequences are listed in Table 1. Synthesis of these primers and probes were conducted by Beijing Genomics Institute (BGI).

**Conduct of dPCR**

The dPCR experiments were conducted using BioDigital Z200 series dPCR platform and the accompanying universal dPCR kit (Saint Genomics, China). The reaction solution consists of 3.5 μL 10 x dPCR buffer, 1 μL polymerase, 1.2 μL 10 μM primers (each), 1 μL 10 μM probes (each), 15.3 μL nuclease-free water, and 5 μL sample genomic DNA (35 μL in total). The solution was placed in the loader machine, where it would be further injected into a microfluidic chip and be separated by the little chambers within to over 20,000 replicates. A following injection of oil mixture would form a thin film over these chambers to protect vapor and cross-contamination. The chips would then be heated by the thermal cycler. The reaction program starts at a curing step for the oil mix: 50℃ for 10 minutes. Then, temperature goes up to 95℃ for another 10 minutes in order to hot-start the Taq polymerase and pre-degenerate the DNA duplex. A two-step amplification process follows: degeneration at 95℃ for 20 seconds and annealing at 57℃ for 40 seconds, lasting for 55 cycles till the end, when the machine would hold at 25℃. After amplification, the chips would be transferred to the reading machine. Three channels of fluorescence signals emitted by each replicate would be detected here. The genomic *TP53* copy number (CN) of a given sample would be calculated as:

$$2 \times \frac{CN\ of\ ChF}{CN\ of\ ChC}\ or\ 2 \times \frac{CN\ of\ ChH}{CN\ of\ ChC}$$

where ChF, ChC, and ChH stand for channel FAM, channel CY5, and channel HEX (detecting the fluorescence emitted by VIC), respectively.

**Karyotyping**

Karyotyping was performed in the laboratory center of our hospital. Samples were directly inspected or cultivated shortly (less than 72 hours) without phytohemagglutinin. Inspections were based on heat-denatured Giemsa R-bandings (RHG-bandings) analysis.

**Next generation sequencing**

NGS tests were conducted by two external laboratories: Uniwell Medical Laboratory and KingMed Diagnostics. The average sequencing depth was 1,000 - 2,000 ×. CNV statuses were included in part of these reports and were not always quantified.

**Statistics**

Statistical analysis in this article was assisted by IBM SPSS Statistics v26.0 and Graphpad Prism v10.1. Calculation of LOBs and LODs followed the formulae given by EP17-A. LOBs were calculated as: $\mu_B \pm 1.645\ \sigma_B$ ($\mu_B$ and $\sigma_B$ are the mean and standard deviation of blank samples, respectively). LODs were calculated as: LOB - $C_\beta SD_p$, while $C_\beta$ = 1.645 / (1-1/ (4 x f)), $SD_p^2 = (n_1SD_1^2 + n_2SD_2^2 + n_3SD_3^2) / (n_1 + n_2 + n_3)$ (f is the degree of freedom of $SD_p$. $n_1$, $n_2$, and $n_3$ are the number of tests conducted on the different levels of low concentration samples. $SD_1$, $SD_2$, and $SD_3$ are the standard deviations of the test results for three levels of low concentration samples respectively. $SD_p$ stands for the pooled standard deviation).

## RESULTS

**Fluorescence separation tests**

The fluorescence separation between positive and negative partitions is a basic criterion when judging the performance of a dPCR method. Figure 1 depicts the 2D and 1D plot results of a single test. Intervals between the positive and negative partitions are spatial while almost no fluorescence leak between various channels can be seen, revealing the excellent separability performance of this assay.

**Establishment of critical values and linearities**

The 102 samples from non-tumor healthy checkup individual's peripheral blood were tested to establish the LOB of this method. Figure 2 depicts the test results of these blank samples. The lower LOB of the two exons were revealed to be 1.756 and 1.836 copies per genome respectively, while the upper limits were 2.008 and 2.041. Notice that there are several results slightly exceeding the limits of blank. This is because the formulae we quoted and used from EP17-A allows for a false positive rate of 5%. The space between LOB and LOD is therefore deemed grey interval. One can choose to reduce the false positive rate to 1% by enhancing the LOB to 2.326 $\sigma_B$ from $\mu_B$, or retest the samples, or use the cutoff values that will be narrated below. When retested, so long as the sample's mutation concentration is

**Table 1. The designed sequences involved in the detection assay.**

| Name | Sequence |
|---|---|
| ***TP53*-exon 5-Forward Primer** | **5'-TACTCCCCTGCCCTCAA -3'** |
| ***TP53*-exon 5-Reverse Primer** | **5'-CTGCTCACCATCGCTATCT -3'** |
| ***TP53*-exon 5-Probe** | **5'-FAM-TGGTGGGGGCAGCGC -BHQ1-3'** |
| ***TP53*-exon 7-Forward Primer** | **5'-AGGTTGGCTCTGACTGTA -3'** |
| ***TP53*-exon 7-Reverse Primer** | **5'-GTGATGATGGTGAGGATG -3'** |
| ***TP53*-exon 7-Probe** | **5'-VIC-CAACTACATGTGTAAC-MGB-3'** |
| ***RPP30*-Forward Primer** | **5'-TGGCTTTTGAACTTGTCT -3'** |
| ***RPP30*-Reverse Primer** | **5'-AACCATACCTTTCCTTTG -3'** |
| ***RPP30*-Probe** | **5'-CY5-ACCTTCTCATTGTGGAGTCTT-BHQ3-3'** |

**Table 2. Characteristics of LOD.**

| Target | $n_1$ | $SD_1$ | $n_2$ | $SD_2$ | $n_3$ | $SD_3$ | $SD_p$ | LOD for CN loss |
|---|---|---|---|---|---|---|---|---|
| **Exon 5** | **6** | **0.020** | **7** | **0.051** | **7** | **0.031** | **0.037** | **1.692** |
| **Exon 7** | **6** | **0.021** | **7** | **0.040** | **7** | **0.035** | **0.034** | **1.777** |

**Table 3. Comparison between results of dPCR and NGS.**

| dPCR | NGS | | Total |
|---|---|---|---|
| | + | - | |
| + | **3 (7)** | **2** | **5 (9)** |
| - | **0** | **11** | **11** |
| **Total** | **3 (7)** | **13** | **16 (20)** |

**The numbers in the brackets indicate the comparison results under the hypothesis that samples reported to bear a *TP53* mutation frequency over 50% could also be regarded as NGS-CNV-positive when dPCR reveals positive CNV results.**

**Table 4. Comparison between results of dPCR and karyotyping.**

| dPCR | Karyotyping | | Total |
|---|---|---|---|
| | + | - | |
| + | **2** | **11** | **13** |
| - | **0** | **22** | **32** |
| **Total** | **2** | **33** | **35** |

beyond the LOD we claimed, there should be at least a 95% chance that the result is still positive. Three out of these 102 samples were randomly chosen, mixed together, and mingled with the DNA of leukemia cell line SKM-1 in 3 different ratios (20%, 30%, and 40% of SKM-1 DNA respectively as the final concentrations in the mixed samples) to simulate the low concentration samples in the real test scenarios. The mimics were re-

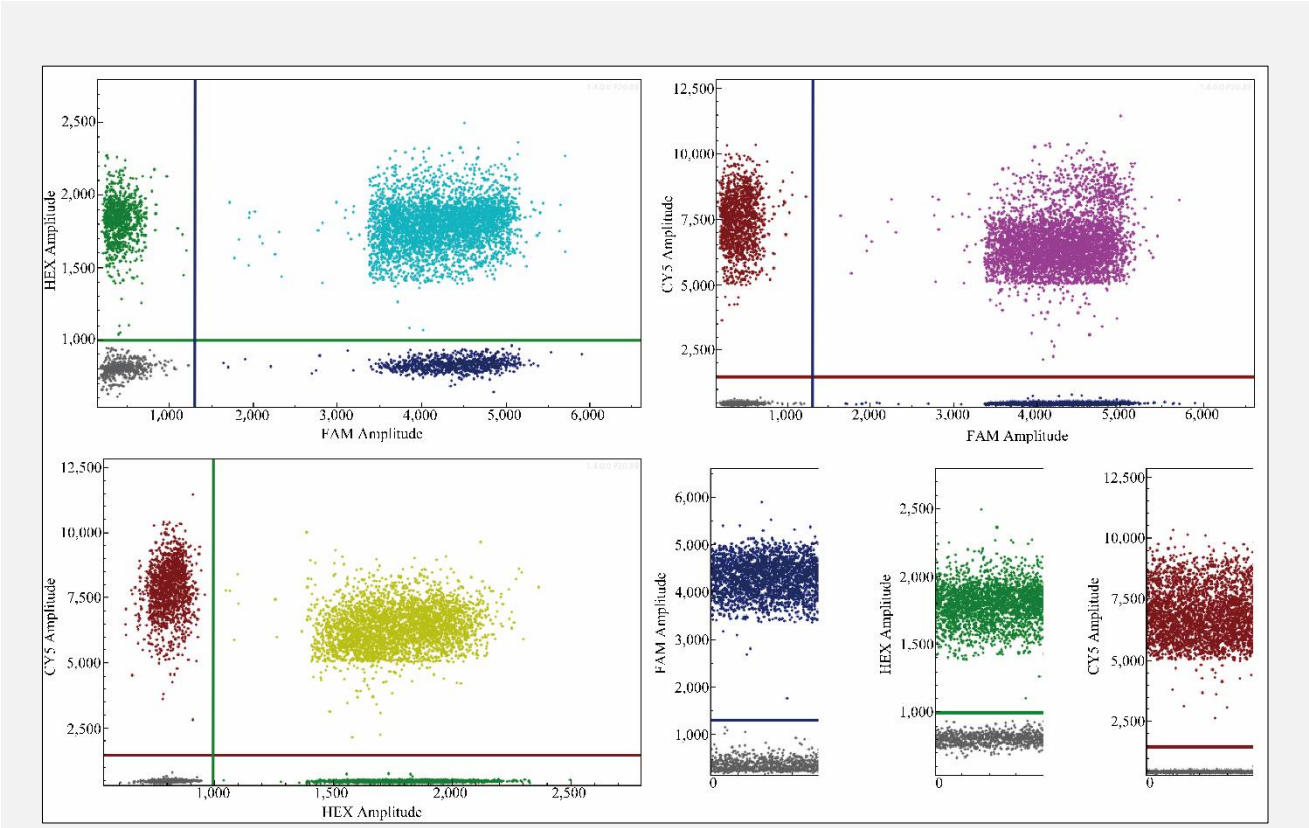


**Figure 1. The 2D and 1D plot results of a single test.**

peatedly tested 20 times. Properties concerning LOD are listed in Table 2. The aforementioned 3 samples from healthy donors were also mixed and mingled with the DNA of the cell line HL-60 at 5 different ratios as the reference materials for the test of the linearity properties of this method (5%, 25%, 50%, 75%, and 100% of HL60 DNA as the final concentrations). The sample at each ratio was tested three times. Results are shown in Figure 3. Spearman correlation coefficients (r) of 0.9971 and 0.9990 for exon 5 and exon 7, respectively, reveal the excellent correlation between the response value and the tested materials.

**Validation of sensitivity**

Twenty-two tests of the samples at the exact concentration of the LOD level for each of the two exons on *TP53* were conducted in two days to verify the sensitivity and coefficients of variation (CV) of this method. Results were listed in the Supplementary Table S1. Both exons have one test result that failed to pass the LOB. This result coordinates with the false negative rate decided by the LOD calculation method that we quoted from EP17-A. The validation of sensitivity was therefore passed. CV for detection of exon 5 was determined as 4.6%, while CV for exon 7 was 2.8%.

**Detection of the samples from newly diagnosed patients**

Forty-two samples from newly diagnosed patients with hematologic malignancies were tested. The test results of each sample and the corresponding clinical information are listed in Supplementary Table S2. Detailed karyotyping results are listed in Supplementary File S3. Among these patients, 30 were also detected with targeted NGS. CNV statuses were only reported in 16 of them. A comparison between the results of NGS tests and our experiments is listed in Table 3. Taking the NGS test as reference standard, we drew the receiver operating characteristic curves (ROC) (Figure 4) to further compare the sensitivity and specificity of dPCR with NGS in detecting CN loss and to establish the cut-off values as another choice of CN loss determination. The figures were drawn under the hypothesis that samples reported to bear a *TP53* mutation frequency over 50% (single, not additive) could also be regarded as NGS-CNV-positive when dPCR reveals positive CNV

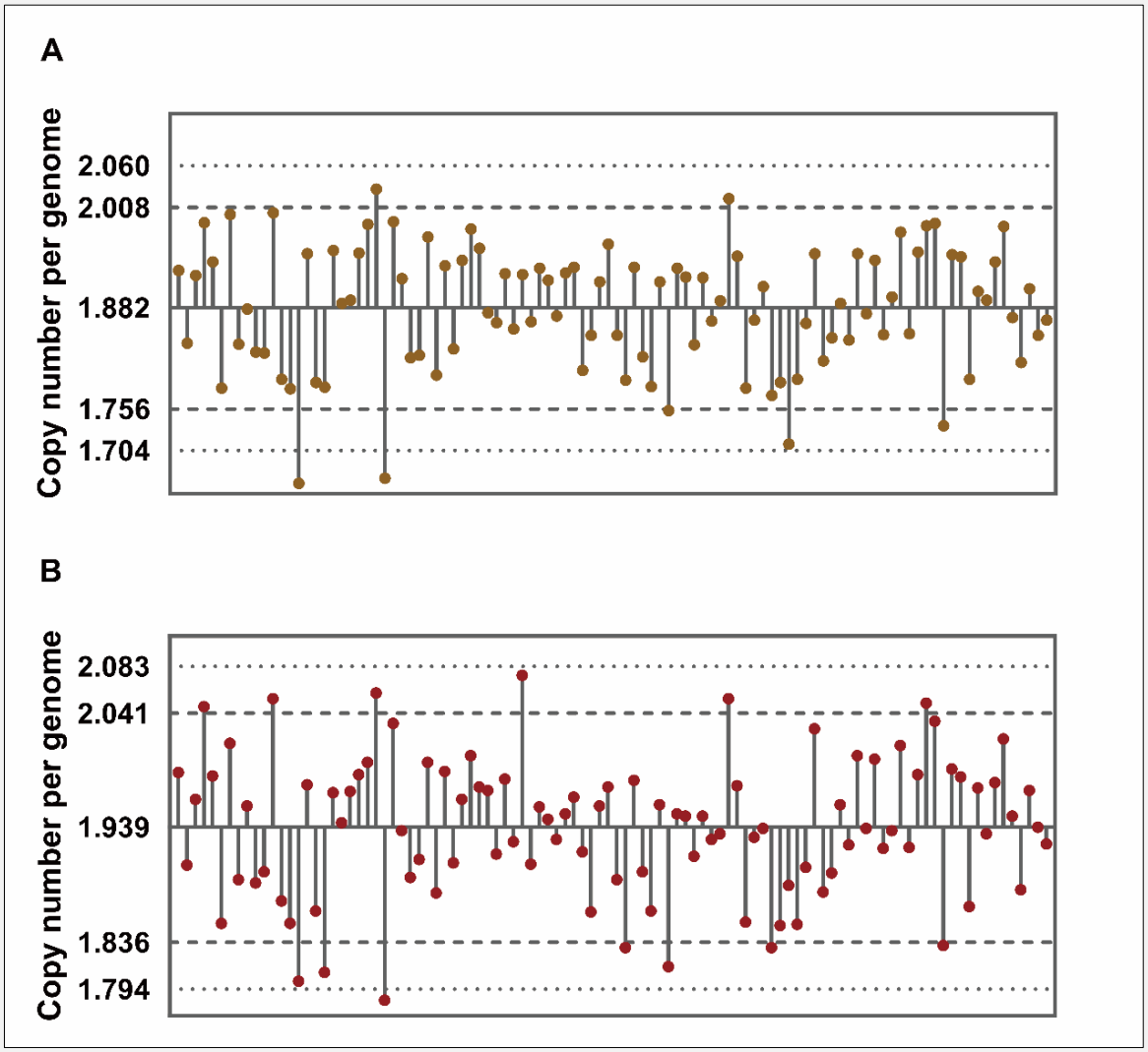


**Figure 2. The test results of healthy checkup individuals.**

**A) Results of the exon 5. B) Results of the exon 7. Each stick represents the result of one sample. The dashed lines in each figure indicate the LOBs (1.645$\sigma_B$ from $\mu_B$) for CN loss and CN gain, while the dot lines in each figure indicate the numbers of 2.326 $\sigma_B$ from $\mu_B$.**

results. It turned out that the areas under curve (AUC) reached 1 for both exons. The cutoff values decided by the ROCs are 1.716 and 1.786 copies per genome respectively for exon 5 and exon 7, which are between the LOB and LOD of the corresponding exon. Karyotypes were reported in 35 patients. The comparison between dPCR and karyotyping is listed in Table 4. Among the 2 patients which were reported CNV positive both by dPCR and karyotyping, the results were actually opposite for the sample ranked the 18th. Karyotyping revealed loss of the chromosome 17, while dPCR showed positive for CN gain, which was consistent with NGS.

## DISCUSSION

In this study, we successfully established a dPCR method for identifying the *TP53* CNV in hematologic malignancy samples. The performance characteristics of this method have been tested and verified to be suitable for CNV screening. For patients having difficulties affording a NGS test or SNP array test, this is a much more affordable choice to make explicit whether they bear *TP53* CNV or not. For physicians in need of fitting in those new diagnostic systems, this method can help them to confirm whether multi-hit or *biTP53* mutations exist.

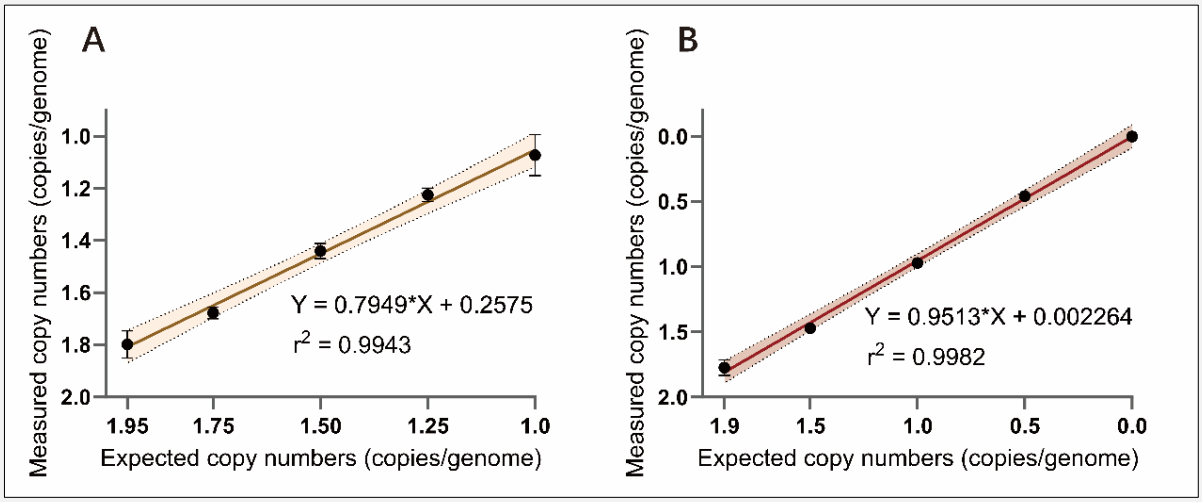


**Figure 3. Linearity properties of the tests.**

**A) Linearity property of the test on exon 5. B) Linearity property of the test on exon 7.**

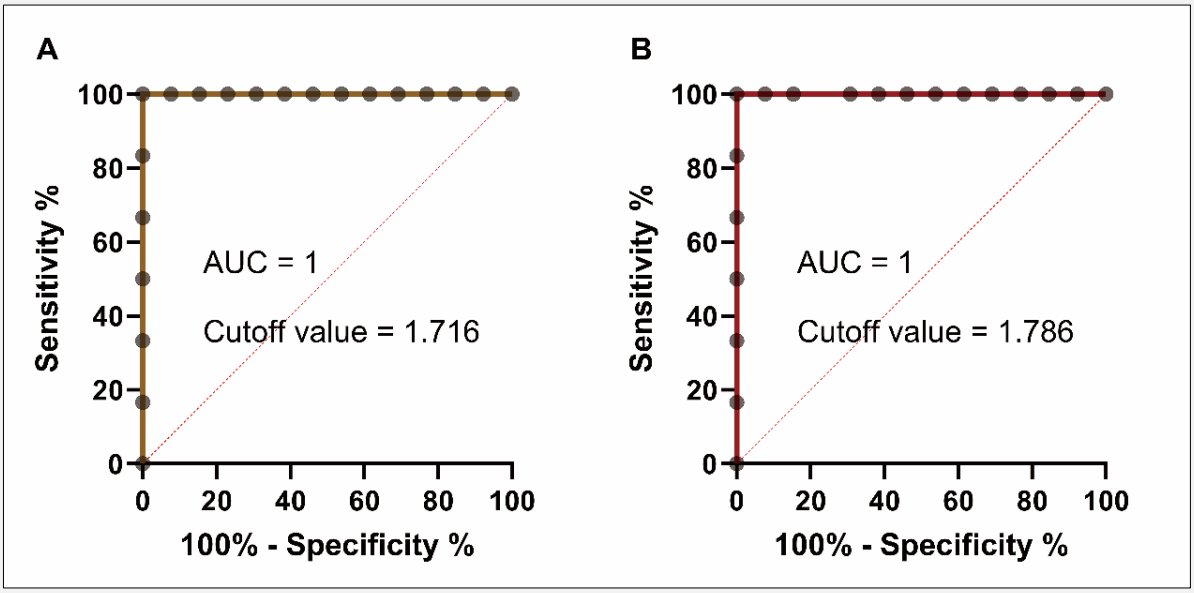


**Figure 4. ROCs of the experiment results.**

**A) ROC of the results of exon 5. B) ROC of the results of exon 7.**

The comparison between the results of our experiments and NGS tests reveals the non-inferior sensitivity of our method in detecting *TP53* CNV. The patient that ranked 29th in Table 3 was found to have no *TP53* mutation or CNV by NGS method, and hence would be diagnosed as MDS-*SF3B1* according to the 2022 WHO classification, which indicates a favorable prognosis. But our experiments revealed that he was positive for *TP53* CNV, even though the variation frequency was relatively low. This surely provided a different expectation on his prognosis. Also, the comparison between our experiments and the traditional karyotyping results revealed the dPCR's obvious superiority of sensitivity in detecting CNV. It is far less than adequate to base our judgement of the genes' CNV statuses on this traditional visual inspection. Digital PCR can, therefore, serve as a powerful supplement. Also, our experiments on newly diagnosed patients' samples narrated above have found *TP53* CNV positive in 11 patients whose NGS reports did not include CNV findings or who did not attend the NGS tests. The method can help us retrospectively test the samples that are preserved in good condition in order to exclude the possibility of *biTP53* mutations, especially when we start to fit in these new diagnostic systems.

When comparing with qPCR, dPCR has a tremendous advantage in the sensitivity of CNV detection, though it may seem to be not as impressive as its performance in the aspect of SNP detection [16-18]. The uncertainty of measurement, which fundamentally decides the sensitivity of a detection method, mainly comes from two aspects: random error and systematic error. For the detection of CNV with a dPCR method is based on the ratio of at least two genes which usually locate on different chromosomes, any factor causing the random error within the detection of a single gene would therefore be enlarged when the results are pooled together [19]. Also, Suzanne and Simant et al. have successfully established the mathematical error model for CNV detection with dPCR method [20,21]. A dPCR test nowadays typically involves approximately 20,000 partitions. Based on their theory, the random error caused by the probability distribution of the proportions of positive partitions on a test chip are still too large to be neglected on such a partition scale. Systematic errors are also displayed in our experiment results, revealed by the mean copy numbers of blank samples being tested. As far as we consider, although the test result of a single droplet in the dPCR test is dichotomous, the slight difference between the amplification efficiencies of the target templates would cause those sequences with relatively low amplification efficiencies to 'drop-out' from the amplification process at the very beginning, as is often seen in those amplification processes with extreme low template concentrations, and so cause the reaction droplet to be deemed as negative, and in the end, cause the systematic errors that are displayed in our results [22]. By optimizing the conditions related to the reaction, we managed to minimize its influence. Yet under this circumstance, the LOB and LOD determined above must be recognized as the response values given by the PCR machine instead of the real concentrations of the samples being tested. One may consider using the linear functions to calibrate the response values as is described in ISO11843-2. This is in essence eliminating the systematic errors by adding the random errors within the process of determining the linear functions into the system. This method calls for more authenticated reference materials; and considering that there were only three replicates for each reference state, the total uncertainty of measurement could even be larger than before calibration. As is demonstrated above, we have validated the detection ability of this method at the exact concentration on the LOD levels and will still hold on to that claim. Deciding whether a test result is positive or not based on linear calibration is not recommended, yet using this calibration to determine the absolute copy number of a tested sample remains a choice for future users.

Though the assay of this test has been optimized, several methods could still be applied to further enhance the detection ability. For example, multiple replicates can be used and pooled together to increase the partition number of a single test. Multiple target loci can be involved within the same reaction assay and separated by the difference between fluorescence intensities [23]. Multiple reference loci can be developed instead of using a single references gene [24]. However, these methods are at present intricate to put into practical use and may still rely on the development of more advanced software to come into assistance in the future.

**Source of Funds:**

This research was supported by the National Natural Science Foundation of China (82270179), Zhenjiang Clinical Research Center of Hematology (SS2018009), Social Development Foundation of Zhenjiang (SH2023 022 and SH2024001), and the Scientific Research Project of The Fifth 169 Project of Zhenjiang (21).

**Declaration of Interest:**

The authors declare that they have no conflicts of interest. There is no involvement of a pharmaceutical/other company.

**References:**

1. Notini AJ, Craig JM, White SJ. Copy number variation and mosaicism. Cytogenet Genome Res 2008;123(1-4):270-7. (PMID: 19287164)

2. Redon R, Ishikawa S, Fitch KR, et al. Global variation in copy number in the human genome. Nature 2006;444(7118):444-54. (PMID: 17122850)

3. Liu Y, Chen C, Xu Z, et al. Deletions linked to TP53 loss drive cancer through p53-independent mechanisms. Nature 2016; 531(7595):471-5. (PMID: 26982726)

4. Tashakori M, Kadia T, Loghavi S, et al. TP53 copy number and protein expression inform mutation status across risk categories in acute myeloid leukemia. Blood 2022;140(1):58-72. (PMID: 35390143)

5. Mikhail FM, Biegel JA, Cooley LD, et al. Technical laboratory standards for interpretation and reporting of acquired copy-number abnormalities and copy-neutral loss of heterozygosity in neoplastic disorders: a joint consensus recommendation from the American College of Medical Genetics and Genomics (ACMG) and the Cancer Genomics Consortium (CGC). Genet Med 2019; 21(9):1903-16. (PMID: 31138931)

6. Arber DA, Orazi A, Hasserjian RP, et al. International Consensus Classification of Myeloid Neoplasms and Acute Leukemias: integrating morphologic, clinical, and genomic data. Blood 2022; 140(11):1200-28. (PMID: 35767897)

7. Khoury JD, Solary E, Abla O, et al. The 5th edition of the World Health Organization Classification of Haematolymphoid Tumours: Myeloid and Histiocytic/Dendritic Neoplasms. Leukemia 2022;36(7):1703-19. (PMID: 35732831)

8. Bernard E, Tuechler H, Greenberg PL, et al. Molecular International Prognostic Scoring System for Myelodysplastic Syndromes. NEJM Evid 2022;1(7):EVIDoa2200008. (PMID: 38319256)

9. Cassinari K, Quenez O, Joly-Hélas G, et al. A Simple, Universal, and Cost-Efficient Digital PCR Method for the Targeted Analysis of Copy Number Variations. Clin Chem 2019;65(9):1153-60. (PMID: 31292136)

10. Bubner B, Gase K, Baldwin IT. Two-fold differences are the detection limit for determining transgene copy numbers in plants by real-time PCR. BMC Biotechnol 2004;4:14. (PMID: 15251044)

11. Hindson BJ, Ness KD, Masquelier DA, et al. High-Throughput Droplet Digital PCR System for Absolute Quantitation of DNA Copy Number. Anal Chem 2011;83(22):8604-10. (PMID: 22035192)

12. Huggett JF; dMIQE Group. The Digital MIQE Guidelines Update: Minimum Information for Publication of Quantitative Digital PCR Experiments for 2020. Clin Chem 2020;66(8):1012-29. (PMID: 32746458)

13. Tholen DW, Linnet K, Kondratovich M, et al. Protocols for Determination of Limits of Detection and Limits of Quantitation; Approved Guideline. NCCLS document EP17-A 2004. https://www.semanticscholar.org/paper/Protocols-for-Determination-of-Limits-of-Detection-Tholen-Linnet/9afc36c690cfbf76f9251464045564a5ee073d7b

14. Hasserjian RP. Revealing the dark secrets of TP53-mutated AML. Blood 2022;140(1):8-10. (PMID: 35797016)

15. Wu J, Yu S, Wang Y, Zhu J, Zhang Z. New insights into the role of ribonuclease P protein subunit p30 from tumor to internal reference. Front Oncol 2022;12:1018279. (PMID: 36313673)

16. Jin Y, Xu Z-J, Yu D, et al. Detection of NPM1 Mutations in Acute Myeloid Leukemia by using Drop-Off Droplet Digital PCR and its Clinical Application. Clin Lab 2023;69(11). (PMID: 37948486)

17. Liu Y, Han C, Li J, et al. Laboratory-developed Droplet Digital PCR Assay for Quantification of the JAK2 V617F Mutation. Global Med Genet 2024;11(2):132-41. (PMID: 38585044)

18. Durgut S, Salihefendić L, Pećar D, et al. Droplet Digital PCR as a Molecular Tool for the Detection of the EGFR T790M Mutation in NSCLC Patients with the EGFR Activating Mutations. Balkan J Med Genet 2024;26(2):21-6. (PMID: 38482255)

19. Farrance I, Frenkel R. Uncertainty of Measurement: A Review of the Rules for Calculating Uncertainty Components through Functional Relationships. Clin Biochem Rev 2012;33(2):49-75. (PMID: 22896744)

20. Dube S, Qin J, Ramakrishnan R. Mathematical Analysis of Copy Number Variation in a DNA Sample Using Digital PCR on a Nanofluidic Device. PLoS One 2008;3(8):e2876. (PMID: 18682853)

21. Weaver S, Dube S, Mir A, et al. Taking qPCR to a higher level: Analysis of CNV reveals the power of high throughput qPCR to enhance quantitative resolution. Methods 2010;50(4):271-6. (PMID: 20079846)

22. Kluwe L. Allelic drop-out, allele imbalance, or loss of heterozygosity? Genes Chromosomes Cancer 2012;51(5):521-2; author reply 523. (PMID: 22294435)

23. Calabrese S, Markl AM, Neugebauer M, et al. Reporter emission multiplexing in digital PCRs (REM-dPCRs): direct quantification of multiple target sequences per detection channel by population specific reporters. Analyst 2023;148(20):5243-54. (PMID: 37727114)

24. Vynck M, Vandesompele J, Nijs N, Menten B, De Ganck A, Thas O. Flexible analysis of digital PCR experiments using generalized linear mixed models. Biomol Detect Quantif 2016;9:1-13. (PMID: 27551671)

**Additional material can be found online at:**
http://supplementary.clin-lab-publications.com/241051/